Space-selective Precipitation and Control of Functional Crystals in Glasses by a Femtosecond Laser

Jianrong Qiu*, Bin Zhu[1], and Ye Dai[2]

[1]*State Key Laboratory of Silicon Materials, Zhejiang University, Hangzhou 310027, China*

[2]*Department of Physics, Shanghai University, Shanghai 200444, China*

**E-mail:qjr@zju.edu.cn*

Abstract: Femtosecond laser micro-processing received much attention in the past decade. The nature of ultra-short light-matter interaction permits femtosecond laser to overcome the diffraction limit and realize precise micro-processing. The ultrahigh light intensity of the femtosecond laser allows sapece-selective microscopic modifications to materials based on multiphoton processes. In this paper, we review our recent research development on space-selective precipitation and control of functional crystals in glasses by an infrared femtosecond laser. The technique will open new possibilities in the fabrication of micro-optical components with various optical functions.

1. Introduction

Femtosecond laser is a powerful tool to make microscopic modifications to glass structure. Compared with CW and long pulsed lasers, femtosecond laser has two apparent features: (1) elimination of the thermal effect due to extremely short energy deposition time, and (2) participation of various nonlinear processes enabled by highly localization of laser photons in both time and spatial domains. Due to the ultra-short light-matter interaction time and the high peak power, material processing with the femtosecond laser is generally characterized by the absence of heat diffusion and, consequently molten layers.[1)] The nature of ultra-short light-matter interaction permits femtosecond laser to overcome the diffraction limit.[2)] The strength of its electric field in the focal point of the laser beam can easlily reach 10TW/cm^2, which is sufficient for inducing various nonlinear physicochemical reactions in glasses by using a focusing lens, when the pulse width is 100fs and the pulse energy is 1μJ. The photo-induced reactions are expected to occur only near the focused part of the laser beam due to multiphoton processes. In the past decade, a lot of research efforts have been devoted to the field of 3 dimensional microscopic modifications to glass materials by using femtosecond laser. Novel phenomena based on nonlinear interaction between femtosecond laser and glasses have been observed,[3-14)] and promising applications have been demonstrated for the formation of 3-dimensional optical memory[3,5,9)] and multicolor image[8)], and fabrication of optical waveguide[4,15)], coupler[16,17)] and photonic crystal[18,19)]. In this paper, we concentrate on space-selective precipitation and control of functional crystals in glasses by an infrared femtosecond laser.

2. Space-selective Precipitation of Nanoparticles

Nanoparticles have a wide range of electrical and optical properties due to the quantum size effect, surface effect and conjoint effect of the nanostructures. Materials doped with noble metal nanoparticles exhibit large third-order nonlinear susceptibility and ultrafast nonlinear response. They are expected to be promising materials for ultrafast all-optical switches in the THz region. For the applications in integrated optoelectronics, a well-defined assembly and spatial distribution of nanoparticles in materials are essential. Many studies have been carried out on fabrications of nanoparticle-

doped materials, but there are no effective methods to control the spatial distribution of nanoparticles in materials. Recently, we realized the space-selective precipitation and control of silver nanoparticles in glasses by using femtosecond laser irradiation and subsequent annealing.[20-22]

2.1 Silver nanoparticles

After irradiation by a focused infrared femtosecond laser at 800nm, a 10 μm spot was formed in the focused area of the laser beam in the Ag^+-doped silicate glass sample. In addition, a gray-colored area with a diameter of about 40 μm was observed around the spot. The glass sample was further annealed at 550℃ for 10 min. The laser-irradiated part became yellow after the heat treatment. No apparent absorption was observed for the unirradiated glass sample in the wavelength region from 600 to 800 nm, while there was an apparent increase in the absorbance in the wavelength region from 220 to 600 nm in the irradiated region.

The difference in absorption spectra of the glass sample before and after the femtosecond laser irradiation shows that there are absorption peaks at about 240 nm and 350 nm, which can be assigned to the atomic silver and hole trap centers at nonbridging oxygen near Ag^+ ions, respectively. Therefore, an electron was driven out from the 2p orbital of a nonbridging atom near the Ag^+ ions after femtosecond laser irradiation, while Ag^+ captured the electron to form an Ag atom. A new peak appeared at 450 nm in the absorption of the glass sample after further annealing at 550℃. The peak can be assigned to the absorption due to the surface plasmon of the silver nanoparticle. Preliminary observation with a JEM-2010FEF transmission electron microscope also showed that spherical particles with sizes ranging from 1 to 8 nm precipitated in the sample. No apparent signal was detected in the electron spin resonance spectrum of the unirradiated glass sample, while the spectrum of the glass sample after femtosecond laser irradiation showed a broad signal at g~2.10 and two signals at g~2.00. The broad signal at 2.10 may be due to the Ag atom, while two signals at g~2.00 can be assigned to hole trap centers (HC), e.g., HC_1 and HC_2. The HC_1 and HC_2 are holes trapped at the nonbridging oxygen in the SiO_4 polyhedron with two and three nonbridging oxygen, respectively. Therefore, the photon-reduced Ag atoms aggregated to form nanoparticles during the heat treatment. An unirradiated glass sample precipitates nanoparticles only at temperatures above 600℃. We suggest that the neutralized Ag acts as crystal nucleus. Femtosecond laser irradiation can be used to separate and control the nucleation and growth processes.

2.2 Gold nanoparticles

Similarly, we can control the precipitation of Au nanoparticles in three-dimension inside transparent materials using focused femtosecond laser irradiation.The precipitation involves two processes: photoreduction of Au ions to atoms induced by multiphoton process and precipitation of Au particles driven by heat treatment. The size of nanoparticles and their spatial distribution can be controlled by the laser irradiation conditions. Interestingly, the precipitated nanoparticles by this technique can be also space-selectively "dissolved" by the femtosecond laser irradiation, and re-precipitated by annealing processes. This implies that the focused femtosecond laser irradiation can be used not only in the practical applications, such as the three-dimensional optical memory and the fabrication of integrated all-optical switches, but also in the study of controlling processes of nucleation and crystal growth.

Gray-colored spots of about 40 mm in diameter were then observed in the focused area through an optical microscope after the femtosecond laser irradiation. No micro-crack was observed in the sample. Annealing at 550℃ for 30 min, these gray-colored spots became red. Using this technique, we first wrote a gray-colored butterfly using the focused femtosecond laser beam,

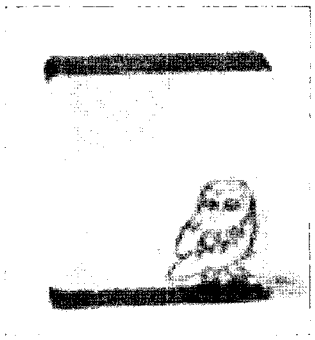

Fig. 1. Photograph of images drawn inside the Au_2O_3-doped silicate glass by using the femtosecond laser irradiation: (a) gray image (without annealing) (b) red image (with annealing).

and then annealed the sample at 550°C for 30 min. The gray-colored butterfly became red. After the sample cooled down to room temperature, we wrote a gray-colored image in the different area of the sample. The images are shown in Fig. 1.

Optical absorption spectra of the 0.01mol%Au_2O_3-doped glass sample before and after femtosecond laser irradiation show that there is an apparent increase in absorbance in the wavelength region from 300 to 800 nm in the irradiated area. The peaks at 245, 306, 430, and 620 nm can be assigned to E' centers, which include an electron trapped in an sp^3 orbital of silicon at the site of oxygen vacancy, hole-trapped by oxygen vacancy neighboring to alkali ions, nonbridging oxygen hole centers HC1 and HC2, respectively.

If the annealing temperature is below 300°C, the absorption (300-800 nm) intensities induced by irradiation decrease as the annealing temperature increases, and completely disappear when the temperatures reaches 300°C. Visually, the femtosecond laser irradiation induced gray color disappears at 300°C and the glass becomes colorless and transparent. Annealing at 450°C results in the appearance of a new peak at 530 nm, and visually the laser-irradiated areas turns into red color. The wavelength of this absorption peak slightly increases with increasing annealing temperature, while its intensity significantly increases.

TEM image showed that nanoparticles precipitated in the femtosecond laser-irradiated 0.01mol%Au_2O_3-doped glass after annealing at 550°C for 30 min. Composition analysis using energy dispersive spectroscopy (EDS) in TEM confirms that these spherical nanoparticles are metallic Au. The size of the Au nanoparticles is ranging from 6 to 8 nm. Therefore, we assign the above absorption peak at 530 nm to the surface plasmon resonance absorption of Au nanoparticles.

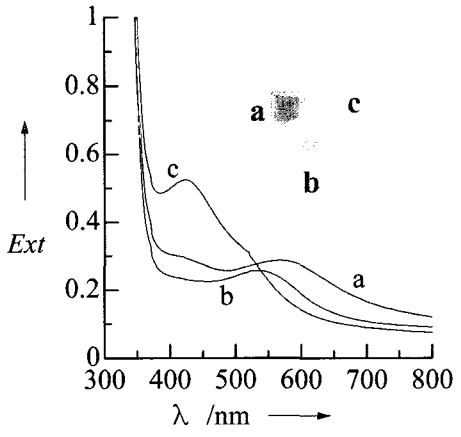

Fig. 2. Extinction spectra of 0.1mol%Au_2O_3-doped glasses irradiated using different light intensities: (a) is 6.5×10^{13} W/cm^2, (b) 2.3×10^{14}, and (c) 5.0×10^{16}. All samples were annealed at 550°C for 1 h. Inset of Fig. 2. Photograph of images drawn inside the 0.1mol%Au_2O_3-doped glass sample.

The inset of Fig. 2 shows the photograph of a 0.1mol%Au_2O_3-doped glass sample, which is irradiated using femtosecond laser beams of 6.5×10^{13}, 2.3×10^{14} to 5.0×10^{16} W/cm^2 in the different areas and then annealed at 550°C for 1 h. With increasing light intensity, the color of the femtosecond laser-irradiated areas became violet, red and yellow, respectively. Fig. 2 shows the extinction spectra from these different colored areas. The extinction peak shifts from 568 to 534 to 422nm with the increase of the light intensity. The peak with the wavelength longer than 500nm observed at spectra a and b, can also be assigned to the surface plasmon resonance absorption of Au nanoparticles. The apparent blue shift of the peak from 568 to 534 nm is due to the decrease in the average size of the Au nanoparticles. An extinction peak is observed at 420 nm in the spectrum c of the Fig. 2. There are few reports on the observation of such peaks in glasses doped with Au nanoparticles. However, the peak position and shape are very similar to those of an undecagold compound with small Au clusters, for example, [Au_{11}]. The peak can be attributed to interband transitions from 5d to 6sp, that is, originating in the submerged and quasicontinum 5d band and terminating in the lowest unoccupied conduction band of the Au clusters. The average size of Au nanoparticles in area c is much smaller than those in areas a and b. Therefore, the average size of the Au nanoparticles decreases with an increase of the light intensity. This is probably because the high irradiation intensity produces a high concentration of reduced Au atoms per unit volume, and thus a high concentration of nucleation centers. As a result, under the same annealing process, the higher the light intensity, the smaller but denser the precipitated particles are.

The reduction of Au ion to atom by femtosecond laser irradiation is the key process of this method. Au ions capture the "free" electrons created by multi-photon process, and are reduced to atoms, which aggregate

Fig. 3. Photographs of images drawn inside the 0.01mol%Au_2O_3-doped glass. (a) using femtosecond laser irradiation and annealing at 550°C for 30 min; (b) further irradiation at the center part of the image in (a) by focused femtosecond laser using a 20x objective lens; (c) then the glass was annealed at 300°C for 300 min.

to form nanoparticles during annealing. During the femtosecond laser irradiation, electrons are driven out of the valence states via the multiphoton absorption of the incident photon. A part of Au ions capture free electrons to form Au atoms. At temperatures below 300°C, only some trapped electrons and holes are excited by thermal energy, and recombine with each other. When annealing at temperatures above 400°C, Au atoms get sufficient energy to overcome the interaction between Au atoms and the glass network structure and start to move apparently. Au nanoparticles form due to the aggregation of Au atoms.

Fig. 3 shows the changes of the Au nanoparticle-precipitated 0.01mol%Au_2O_3-doped glass sample after further femtosecond laser irradiation. Glass sample was first irradiated by the focused femtosecond laser with a light intensity of 5.8×10^{14} W/cm^2 and a scanning rate of 1000 μm/s, and then was annealed at 550°C for 30 min. The laser-irradiated area became red as shown in Fig. 3(a), which has been discussed in the previous paragraphs. Then the laser beam was focused on the center of the nanoparticle-precipitated region and wrote lines with length slightly longer than that of the nanoparticle-precipitated region (Fig. 3(b)). The light intensity and scanning rate were 3.9×10^{14} W/cm^2 and 1000 μm/s, respectively. It is seen that there is a slight change between Fig. 3(a) and (b) due to the formation of color-centers. After the annealing at 300 °C for 30 min, the second femtosecond laser-irradiated part became transparent, which is shown in Fig. 3(c). Interestingly, the transparent part in the center became red after further annealing at 550°C for 30 min. The absorption due to the surface plasmon resonance absorption decreases while the absorption due to the non-bridging oxygen hole centers HC1(430nm) and HC2 (620nm) increases after further laser irradiation. Therefore, we suggest that some precipitated nanoparticles were broken into small size or atoms due to the strong interaction between the Au nanoparticles and ultrashort laser pulses e.g. dramatic heating of nanoparticles due to the linear and nonlinear absorption of laser energy during the further femtosecond laser irradiation.

We also demonstrated the formation of one- dimensional microarrays constituted with Au nanoparticles in Au_2O_3-doped glasses induced by two interfered femtosecond laser pulses followed by successive heat treatment.[23] The spacing and width of the microarrays can be controlled by changing the incident angle between the two interfered pulses and the laser pulse energy. The two incident beams were first focused onto the front surface of Au_2O_3-doped glass to optimize the incident pulse energy. In the case of sufficiently high energy, the two coherent beams can induce periodic ablation, forming a grating in the glass. Herein, we reduced the energy to a certain lower level at which the two coherent beams cannot directly induce periodic ablation, and the grating can only be formed after heat treating the sample at 55°C for 1 h. Such grating was constituted by the laser-heating induced Au nanoparticle precipitation in the Au_2O_3-doped glass. In our experiments, this lower pulse energy was selected to be ~30 and 38 μJ for comparison, and the colliding angle θ between the two incident beams was fixed at ~ 45°.

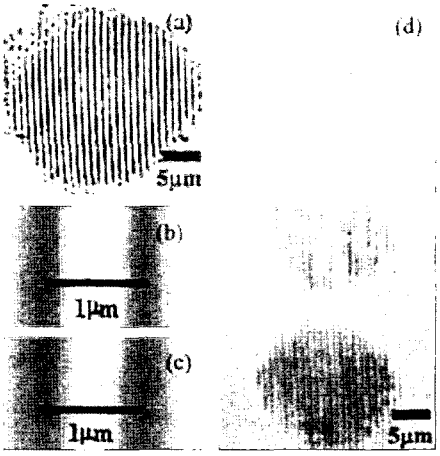

Fig. 4. Optical microscope photographs of Au nanoparticles precipitation in periodic arrays in silica glass, taken by a 100x transilluminated optical microscope. (a) Energy is 30μJ per pulse. (b) Magnified view of (a). (c) Energy is 38μJ per pulse. (d) Part of a group of micrograting.

Fig. 4 shows a part of the new grating. The absorption spectrum of the grating was measured by a spectrophotometer. A weak peak occurs around 508 nm, which is induced by the surface plasmon resonance of An nanoparticles in the glass. The Au nanoparticles with ~3 nm average size in the glass were observed from a transmitted electronic microscopy image. However, we observed neither absorption peak in the range of 500-600 nm as seen, nor Au nanoparticles constituted micrograting in the glass sample irradiated only by the interfered pulses but not heat treated. This indicates that the Au nanoparticles can be precipitated in the periodic one-dimensional arrays in the glass through the irradiation of two coherent beams with the aid of heat treatment.

3. Space-selective Precipitation of Functional Crystals

In the past decades, it has been shown that a femtosecond laser is a powerful tool for micro-fabrication in glass materials. One of the advantages of this method is that the nonlinear absorption only occurs near the focal point of the femtosecond laser beam. If the beam is focused into the glass bulk, the surface is unaffected. In the case of a high repetition rate femtosecond laser, the laser energy is deposited repeatedly in the area of focal point and turned into thermal energy by through the electron-phonon coupling mechanism. This may lead to a temperature rise high enough to induce crystal growth. As a result, the crystallization region can be spatially selected via controlling the focused position of the laser beam. Nonlinear optical crystals have been induced in several glasses using this method.[24-25]

When the laser pulse width is shorter than 10 ps, the high peak power creates a short burst of ionization in the focused area, which subsequently become localized heat. Therefore, during the focused laser irradiation with a high repetition rate, there is a temperature field in the laser focused area. Those parts in the focused area where the temperature exceeds crystallization temperature forms crystal nuclei at first, due to the atomic diffusion and microstructure rearrangement driven by the heat energy. Then, β-BaB_2O_4 (BBO) crystals grow on the nuclei with the passage of time.

The emission spectra obtained from moving the laser focal point accompanies with the growth of frequency conversion crystals. Although only broadening of 800 nm femtosecond laser pulses due to self-phase modulation was observed immediately after laser irradiation, with the passage of time, it was confirmed that the intensity of second harmonic generation increases with the growth of frequency conversion crystals. In addition, after frequency conversion crystals have been created by femtosecond laser irradiation, second harmonic generation of blue beam was observed by the incidence of an infrared nanosecond laser pulse.

Moving the position of the focal point of the laser beam relative to the glass sample enables the heated region to be moved freely. We attempted to generate frequency conversion crystals continuously inside the glass sample by moving the heated zone. The moving speed of the heated zone for region A and B was 100 μm/s and 10 μm/s, respectively. The heated zone was moved continuously from region A to region B. The glass layer situated at the periphery of the grown crystal constitutes an area whose structure has changed due to the crystallization of specific components in the glass. The crystal of region A is clearly a polycrystal due to the existence of grain boundaries revealed by a change in interference color. On the other hand, the crystal of region B exhibits hardly any grain boundaries indicating a crystal having a fixed orientation. The above phenomenon indicates that by decreasing the moving speed of the heated zone, a stable structure having an accommodation layer was formed at the solid-liquid interface between a part of the polycrystal in region A and the heated zone. It means that this technique gives the growth of a single crystal or a crystal with a single-crystal-like structure. By using seed-crystals in the phase matching direction, it is possible to grow crystals adequate for use in frequency conversion devices.

Fresnoite ($Ba_2TiSi_2O_8$) is a ferroelectrics crystal with a very large second-order optical nonlinearity. We also realized space-selective precipitation of $Ba_2TiSi_2O_8$ crystals in a BaO-TiO_2-SiO_2 glass.[26]

Fig. 5 shows photographs around the focal point of the laser beam during femtosecond laser irradiation. At the initial stage of irradiation, a supercontinuum white light was observed, arising from self-phase modulation of the femtosecond laser in the focal point area. After

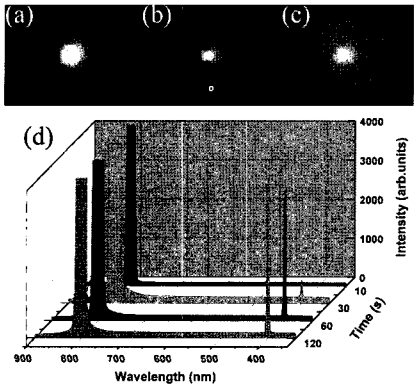

Fig. 5. Photographs around the focal regions during the femtosecond laser 4 irradiation for (a) 10s, (b) 30s, (c) 60s, respectively. (d) Time dependence of 5 second-harmonic generation intensity during the femtosecond laser irradiation.

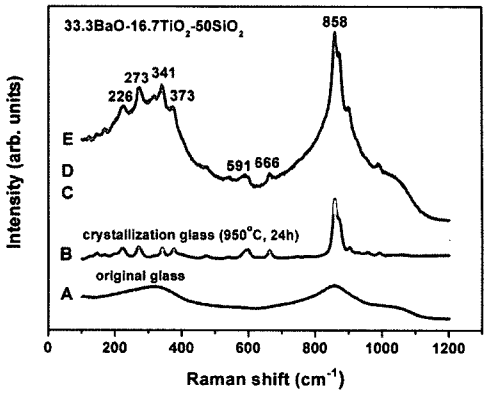

Fig. 6. Micro-Raman spectrum for the original glass (curve A), for the 12 crystallization glass (curve B), and for the femtosecond laser induced-crystallization 13 regions after irradiation for 30s (curve C), 60s (curve D), and 120s (curve E).

30s of irradiation, a bright blue light emerged from the focus region. This phenomenon results from the frequency doubling of the 800 nm incident light, which is due to the laser-induced nonlinear optical effect. The intensity of this 400 nm blue light became stronger and stronger with increasing irradiation.

This may indicate the growth of the frequency-conversion crystals. After 120s of irradiation, the intensity of blue light remained constant, and the crystals stopped growing since the laser-induced thermal field may have reached a balance. After the femtosecond laser irradiation, a circular region was observed at the focal point. The circular regions expanded continuously due to the shock wave and thermal stress at the initial stage of the irradiation. There was no difference in the diameters of the circular regions with femtosecond laser irradiation in the period spanning from 10s to 120s after the start of the iradiation. In view of the high temperature and pressure produced by multiphoton ionization and microexplosion in the focal point, it is reasonable to believe that a part of the laser energy was consumed by the rearrangement of the internal structure due to transition from glass to crystal. In a separate experiment, no crystallization occurred when the glass was irradiated by a 1 kHz femtosecond laser with the same pulse energy and pulse width. Therefore the crystallization may be due to the thermal accumulation effect of the high repetitive rate femtosecond laser. Under cross-polarized light, we also observed colored interference fringes due to formation of crystals near the focal regions. The colors became more and more apparent with increasing irradiation time. The laser-induced crystallization in the glass was also confirmed by micro-Raman spectroscopy. As shown in Fig. 6, the femtosecond laser irradiation induces significant structural changes. In the original glass, the broad band at 837 cm^{-1} can be assigned to the stretching of short Ti-O* bond (O* denotes an apical oxygen), Ti-O- bonds (O- denotes a nonbridging oxygen), and terminal SiO_3 groups, and the band at 290 cm^{-1} are most likely due to the ν(Ba-O) mode. After laser irradiation, the band at 858 cm^{-1} becomes narrower and narrower with increasing irradiation time, while the 290 cm^{-1} band splits into several peaks. The strongest peak at 858 cm^{-1} can be assigned to the vibration of the short Ti-O bond. The peaks at 226, 273, 343 and 373 cm^{-1} are due to the translational and bending modes of the Si_2O_7 and TiO_5 groups. Additionally, two peaks at 591 and 666 cm^{-1} assigned to the ν(TiO_4) and νs(Si-O-Si) modes occur after irradiation, and their intensities increase remarkably with increasing irradiation time. This indicates that the crystal structure consists of the corner-linked TiO_5 pentahedra and pyrosilicate groups Si_2O_7. All these sharp peaks agree with the Raman spectrum of $Ba_2TiSi_2O_8$ single crystal. Therefore, the above results indicate that monophase $Ba_2TiSi_2O_8$ crystals have been induced ithe focal region after femtosecond laser irradiation.

Since the formation mechanism of the induced crystal was similar to zone melting method for crystal growth, we tried to move the focal position of the fem-

tosecond laser continuously inside the glass sample after the frequency-doubled blue light had emerged from a starting position. Interestingly, the emission position of the blue light always followed the focal point when the moving speed of the focal point was 5 μm/s. Therefore, we could write continuous crystal lines inside the glass. This technique can be applied to frequency conversion devices, e.g. three-dimensional displays and nonlinear optical elements.

4. Conclusion

We have observed and discussed the mechanisms of the femtosecond laser induced various localized microstructures in glasses. We demonstrated the possibility of three-dimensional precipitation and control of metal and functional crystals in glasses. The technique will be useful in the fabrication of three-dimensional multicolored industrial art object, rewriteable optical memory with ultrahigh storage density, integrated optical circuit and micro-optical devices.

Acknowledgements

The authors appreciate Professors K. Hirao, K. Miura of the graduate School of Engineering, Kyoto University, Japan, Prof. J. Si of Xian Jiaotong University and Prof. C. Zhu, Drs. X. Jiang, S. Qu and Q. Zhao of Shanghai Institute of Optics and Fine Mechanics, Chinese Academy of Sciences, for their kind cooperation. J.Q. would like to acknowledge the financial support provided by National High-Tech Research and Development Program of China (G20060914).

References

1. Chickov, B. N., Momma, C., Nolte, S., Alvensleben, F. V., Tunnermann, A., Appl Phys A 1996, 63, 109.
2. Pronko, P., Dutta, S., Squier, J., Rudd, J., Mourou, G., Opt Commun 1995, 114, 106.
3. Misawa, H., Japanese Patent Application No. 023614 (1995)
4. Davis, K. M., Miura, K., Sugimoto, N., Hirao, K., Opt Lett 1996, 21, 1729.
5. Glezer, E. N., Milosavljevic, M., Huang, L., Finlay, R. J., Her, T. -H., Callan, J. P., Mazur, E., Opt Lett.,1996, 21, 2023.
6. Qiu, J., Kojima, K., Miura, K., Mitsuyu, T., Hirao, K., Opt Lett 1999, 24, 786.
7. Qiu, J., Miura, K., Suzuki, T., Mitsuyu, T., Hirao, K., Appl Phys Lett 1999, 74, 10.
8. Qiu, J., Zhu, C., Nakaya, T., Si, J., Hirao, K., Appl Phys Lett 2001, 79, 3567.
9. Miura, K., Qiu, J., Fujiwara, S., Sakaguchi, S., Hirao, K., Appl Phys Lett 2002, 80, 2263.
10. Kazansky, P. G., Inouye, H., Mitsuyu, T., Miura, K., Qiu, J., Hirao, K., Starrost, F., Phys Rev Lett 1999, 82, 2199.
11. Qiu, J., Kazansky, P. G., Si, J., Miura, K., Mitsuyu, T., Hirao, K., Gaeta, A. L., Appl Phys Lett 2000, 77, 1940.
12. Shimotsuma, Y., Kazansky, P. G., Qiu, J., Hirao, K., Phys Rev Lett 2003, 91, 247405.
13. Watanabe, W, Toma, T., Yamada, K., Nishii, J., Hayashi, K., Itoh, K., Opt Lett 2000, 25, 1669.
14. Kanehira, S., Si, J., Qiu, J., Fujita, K., Hirao, K., Nano Lett 2005, 5, 1591.
15. Miura, K., Qiu, J., Inouye, H., Mitsuyu, T., Hirao, K., Appl Phys Lett 1997, 71, 3329.
16. Homoelle, D., Wielandy, S., Gaeta, A. G., Borrelli, N. F., Smith, C., Opt Lett 1999, 24, 1311.
17. Minoshima, K., Kowalevicz, A. M., Hartl, I., Ippen, E. P., Fujimoto, J. G., Opt Lett 2001, 26, 1516.
18. Sun, H., Xu, Y., Joudkazis, S., Sun, K., Watanabe, M., Nishii, J., Matsuo, S., Misawa, H., Opt Lett 2001, 26, 325.
19. Wong, S., Deubel, M., Perez-Willard, F., John, S., Ozin, G. A., Wegner, M., Freymann, G. V., Adv. Mat 2006, 18, 265.
20. Qiu, J., Shirai, M., Nakaya, T., Si, J., Jiang, X., Zhu, C., Hirao, K., Appl Phys Lett 2002, 81, 3040.
21. Qiu, J., Jiang, X., Zhu, C., Inouye, H., Si, J., Hirao, K., Opt Lett 2004, 29, 370.
22. Qiu, J., Jiang, X., Zhu, C., Shirai, M., Si, J., Jiang, N., Hirao, K., Angew Chem Int Ed 2004, 43, 2230.
23. Qu, S., Qiu, J., Zhao, Q., Jiang, X., Zeng, H., Zhu, C., Hirao, K., Appl Phys Lett 2004, 84, 2046.
24. Miura, K., Qiu, J., Mitsuyu, T., Hirao, K., Opt Lett 2000, 25, 408.
25. B. Yu, B. Chen, X. Yang, J. Qiu, X. Jiang, C. Zhu, K. Hirao, J. Opt. Soc. Am. B **21**, 10 83 (2004).
26. Dai, Y., Zhu, B., Qiu, J. Ma, H. , Lu, B., Cao, S. , Yu, B. , Submitted.
27. S. A. Markgraf, S. K. Sharma, A. S. Bhalla, J. Mater. 1 Res. 8, 635 (1993).